2021 IEEE Applied Power Electronics Conference and Exposition (APEC) | 978-1-7281-8949-9/21/$31.00 ©2021 IEEE | DOI: 10.1109/APEC42165.2021.9487251

Integrated On-line EIS Measurement Scheme Utilizing Flying Capacitor Equalizer for Series Battery String

*Phuong-Ha La and **Sung-Jin Choi
Department of Electrical, Electronic and Computer Engineering
University of Ulsan, Ulsan 44610, Korea
**laphuongha@gmail.com, **sjchoi@ulsan.ac.kr*

***Abstract*—In the electric vehicle and the battery energy storage systems, hundreds of battery cells are connected in series to reach the voltage requirement. Since the battery degradation can be assessed by the change in battery impedance, online impedance spectroscopy for individual cell are required. While conventional methods require an extra circuitry increasing the system cost, this paper proposes an online electro-chemical impedance spectroscopy (EIS) scheme that can be easily integrated into the switch-matrix flying capacitor equalizer. The real-time simulation shows that the measurement error within 5% is achieved for cell impedance by the measuring circuit seamlessly integrated into the series equalizer.**

***Index Terms*—Battery impedance measurement, online EIS, switch-matrix flying capacitor, series battery string.**

I. Introduction

In the electric vehicle (EV) and the battery energy storage system (BESS), hundreds of battery cells are connected as a series string. Although battery cells are screened before assembling, their performances can be dissimilar, which may lead to over-charging or over-discharging issue for the battery system. Thus, state-of-charge (SOC) and state-of-health (SOH) of individual battery cells should be estimated for a better protection in addition to the cell voltage monitoring. In theory, the SOH of the battery can be assessed either by the change in the maximum available capacity or the degradation of battery impedance. However, because the full capacity only can be observed at the end of the charging and the discharging process, it is more realistic to estimate the SOH by the degradation of battery impedance. Among various impedance estimation methods that have been listed in [1], the online electro-chemical impedance estimation utilizing the existing cell balancing circuit is more promising in the view of practical feasibility and economic consideration.

In [2] and [3], a charger circuitry is utilized to inject an AC signal to a battery cell/pack and the battery impedance is estimated at the end of the charging process based on the measured battery voltage and current. However, this method only estimates the impedance of the whole battery pack at one time and the waiting time for the next measurement is too long to gain timely information. On the other hand, a switched-inductor converter is used to equalize the energy

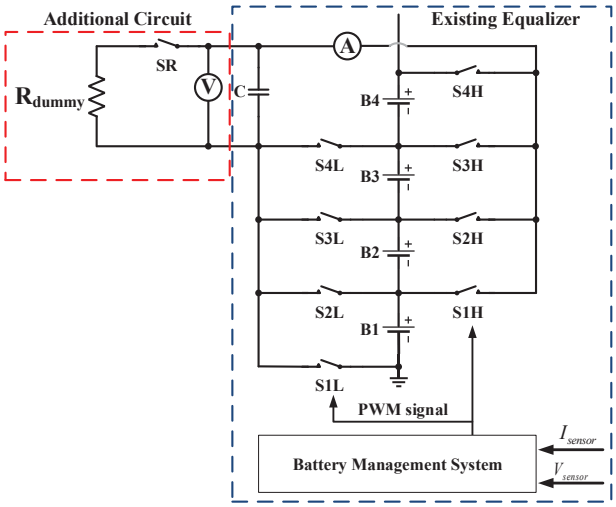

Fig. 1: Proposed integrated measuring circuitry

between two adjacent battery cells, and the balancing voltage waveform is utilized as an injecting AC signal for electro-chemical impedance measurement [4]. However, the measured data have to be processed on MATLAB, which is impractical in actual applications. Similarly, an online impedance spectroscopy using the switched-capacitor cell balancing method is proposed in [5], where the battery impedance is estimated with high accuracy by changing the switching frequency. Although it is one of the most promising methods due to its high efficiency and speed, the accuracy is reduced when the SOC levels of cells are almost equalized. Besides, an extra pair of current-voltage sensors is required to estimate the impedance of two adjacent cells, which reduces its practical feasibility. Thus, an EIS measurement scheme that has high efficiency and speed but low-cost is required.

To mitigate these limitations, this paper proposes an online impedance estimation scheme for individual battery cells in a series string. The proposed method utilizes a switch-matrix flying capacitor equalizer suggested in [6]. The operation principle is introduced in Section 2, real-time simulation

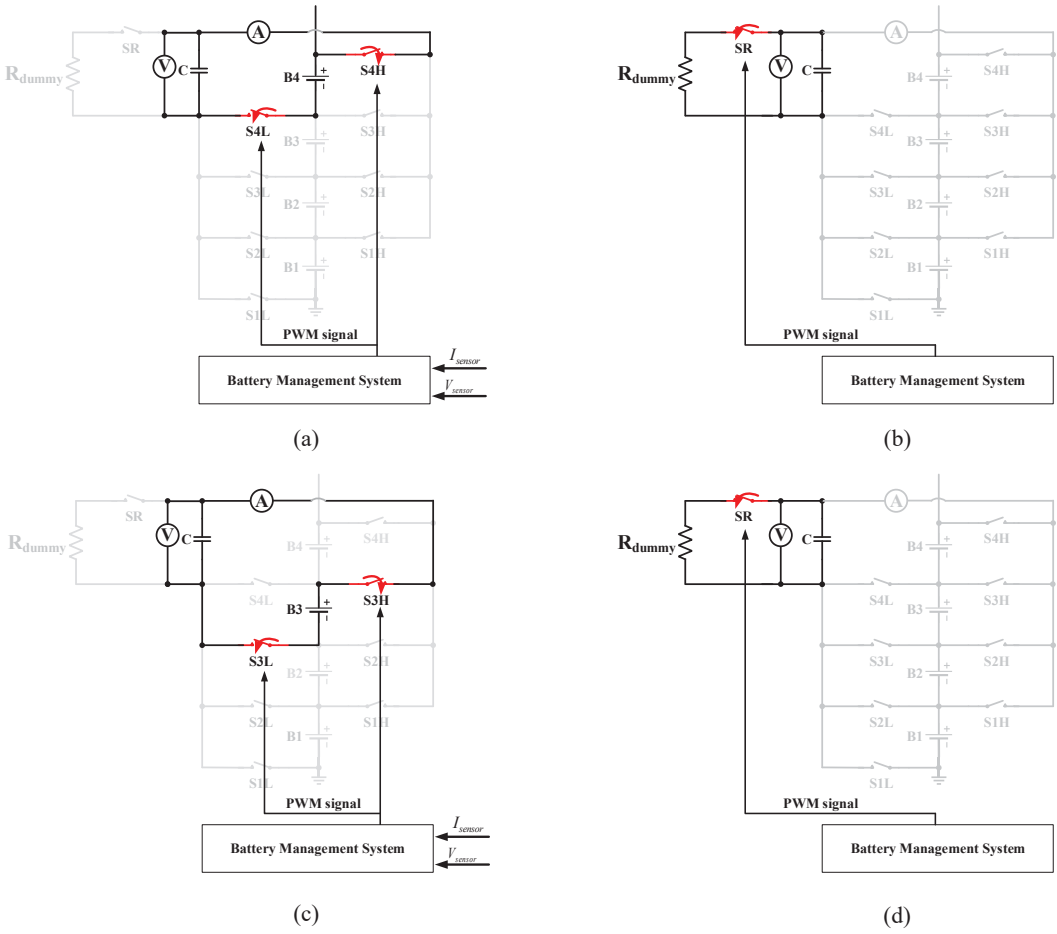

Fig. 2: Operating principle: (a) phase A of cell #4; (b) phase B of cell #4; (c) phase A of cell #3; (d) phase B of cell #3.

results are presented in Section 3, and the conclusion is made in Section 4.

II. Propose Method

A. Proposed Integrated Measuring Circuitry and Operating Principle

The proposed online EIS measuring scheme can be easily embedded into the switch-matrix flying capacitor equalizer to measure the EIS of the individual battery cell. Only an extra voltage sensor to measure the capacitor voltage and one switch-resistor pair to completely discharge the capacitor is required during each measurement as in Fig. 1. During the normal cell balancing operation, those added circuits are inactive. When it is necessary to update the battery impedance status, the measuring circuit becomes active.

The impedance of battery cells is alternately measured one cell at a time. The measuring process of one cell is divided into two phases. During phase A, the first battery (cell $\#4$) is connected to the capacitor, C, as in Fig. 2(a). The voltage and current of the capacitor are measured to estimate the battery impedance. The detailed measuring process is discussed in Section II-B. To alleviate the influence of noise, multiple measuring processes are executed and the average value of the battery impedance is calculated. After that, the capacitor is fully discharged (calibration step) by a shunt resistor, R, during phase B as in Fig. 2(b), where the switch S_R is turned on and the other switches are turned off. The capacitor calibration step is essential to ensure the measuring accuracy.

After the measuring process of one cell is finished, the next battery cell is docked into the capacitor, C, and another measuring process is started for the next battery (cell $\#3$) as in Fig. 2(c) and 2(d). When the impedance of all cells are scanned, one cycle of the estimation process finishes and stays ready for the next measurement cycles.

B. Online EIS Measuring Scheme

The EIS measuring scheme is based on the operation principle of the switched-capacitor equalizer and is illustrated as Fig. 3(a). Since the switches are controlled by a complementary PWM signal as in Fig. 3(b), one measuring cycle is divided into 2 phases. To analyze the operation principle, the circuit is transformed into the s-domain as in Fig. 4, where R_n is the total resistance of the loop (sum of on-resistance of the

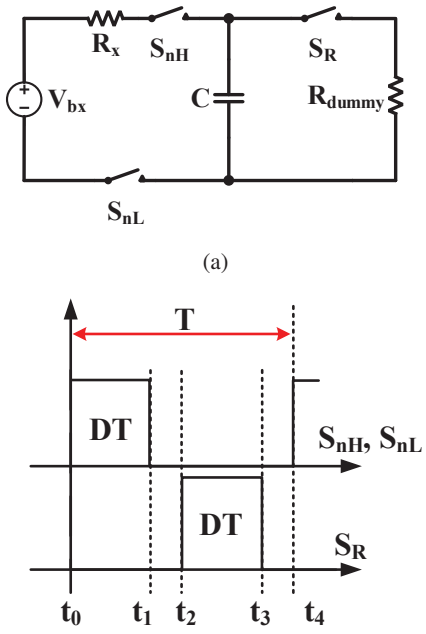

Fig. 3: Simplified circuit for analysis: (a) equivalent circuit of one measuring cycle; (b) control signal.

switch, $R_{d,on}$, the internal resistance of the capacitor, ESR, and the resistance of the cell, R_b), which is given by.

$$R_n = R_{bn} + R_{d,on} + ESR. \tag{1}$$

Besides, C is the capacitance of the balancing capacitor and v_c is the voltage of capacitor. The rising time constant, τ_{1n}, of the switched capacitor in phase A is denoted by

$$\tau_{1n} = R_n C, \tag{2}$$

where n is the index number for the series connected cells.

During phase A ($t_0 \sim t_1$) as in Fig. 4(a), switches S_{nH} and S_{nL} are turned on while the S_R is kept off. The current flowing into the capacitor, $I_1(s)$, is calculated by

$$I_1(s) = \frac{\Delta V}{R_n} \frac{1}{s + \frac{1}{\tau_{1n}}}, \tag{3}$$

where ΔV is the difference between the cell open-circuit voltage and the initial voltage of the capacitor as

$$\Delta V = V_{bn} - v_c(t_0). \tag{4}$$

In time domain, the charging current is expressed as

$$i_1(t) = \frac{\Delta V}{R_n} e^{\frac{-t}{\tau_{1n}}}, \tag{5}$$

and then, the charge increment in the capacitor during phase A is calculated by

$$\begin{aligned} Q_{inc}(t_1) &= \int_{t_0}^{t_1} i_1(t)dt \\ &= C\Delta V \left(1 - e^{\frac{-t_1}{\tau_{1n}}}\right). \end{aligned} \tag{6}$$

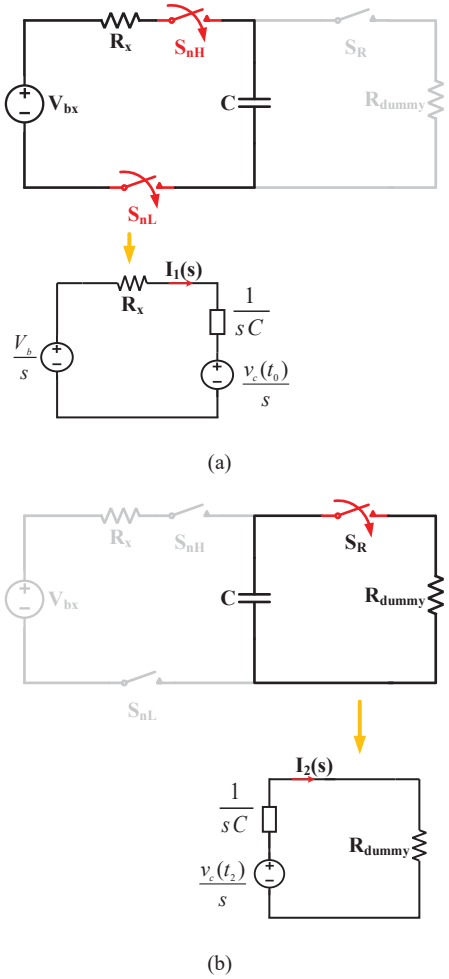

Fig. 4: Equivalent circuit in s-domain: (a) phase A ($t_0 \sim t_1$); (b) phase B ($t_2 \sim t_3$).

As a result, the capacitor voltage at time t_1 is given by

$$\begin{aligned} v_c(t_1) &= \frac{Q_{inc}}{C} \\ &= \Delta V \left(1 - e^{\frac{-t_1}{\tau_{1n}}}\right) + v_c(t_0) \\ &= \Delta V \left(1 - e^{\frac{-t_1}{\tau_{1n}}}\right). \end{aligned} \tag{7}$$

The last equality holds when the initial voltage $v_c(t_0)$ is assumed to be zero, which is guaranteed by phase B operation, calibration step.

After dividing (5) by (7) to eliminate ΔV, a conductance function is obtained as

$$\frac{i(t_1)}{v_c(t_1)} = \frac{1}{R_n} \frac{e^{\frac{-t_1}{R_n C}}}{1 - e^{\frac{-t_1}{R_n C}}}. \tag{8}$$

By denoting G_n as

$$G_n = \frac{1}{R_n}, \tag{9}$$

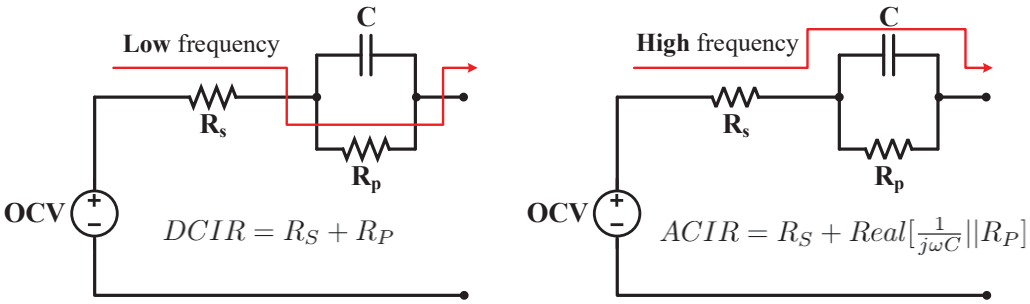

Fig. 5: Battery impedance model: (a) dominant current flow in low frequency operation; (b) dominant current flow in high frequency operation.

we obtain the nonlinear equation

$$f(G_n) = G_n \frac{e^{\frac{-G_n t_1}{C}}}{1 - e^{\frac{-G_n t_1}{C}}} - \frac{i(t_1)}{v_c(t_1)}, \tag{10}$$

which should be equal to zero. From (10), G_n can be obtained by the measurement of the capacitor current, $i_c(t)$, and the voltage, $v_c(t)$, at the end of phase A. Among various numerical algorithms that can be used to find G_n, the Newton-Raphson method is adopted in this paper due to its fast convergence feature. The function is reformulated to

$$G_n(i+1) = G_n(i) \frac{f(Gn(i))}{f'(G_n(i))}, \tag{11}$$

where $f'(G_n(i))$ is the first derivative of $f(G_n(i))$ with respect to G_n, and $G_n(i)$ is the solution in the $i-th$ iteration step. After G_n is calculated, the resistance of battery cell is obtained by

$$R_{bn} = \frac{1}{G_n} - R_{d,on} - ESR. \tag{12}$$

The internal impedance of lithium-ion cell could be represented by various models that are introduced in [7], but the Thévenin model in Fig. 5 is the most popular. According to the model, DCIR could be observed in the low-frequency tests as in Fig. 5(a) or ACIR could be measured in the high frequency examinations as in Fig. 5(b). Technically, by changing the switching frequency, the battery impedance-frequency relationship could be identified.

During phase B ($t_2 \sim t_3$), the capacitor is fully discharged by a dummy load, R_{dummy}, for the next measurement. To ensure completely discharging, the value of the dummy resistance is carefully designed by

$$R_{dummy} \leq \frac{1}{5 f_{s,max}} C, \tag{13}$$

where $f_{s,max}$ is the maximum switching frequency in the test. Because the proposed method utilizes the existing balancing circuit, the design of the capacitance value, C, is not considered in this paper.

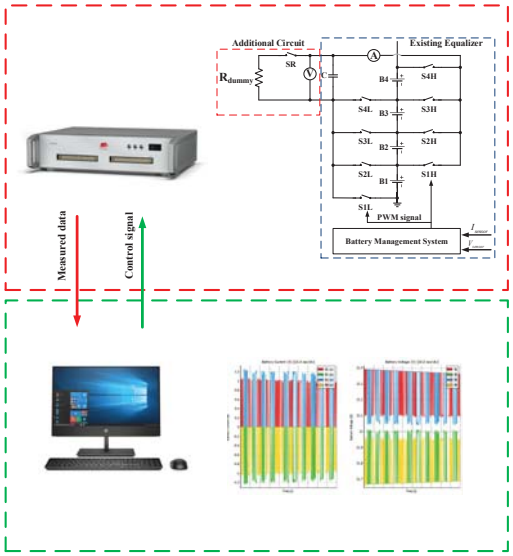

Fig. 6: Real-time simulation setting.

III. Verification

To verify the performance of the proposed method, real-time simulations using four series-connected battery cells ($18650 - 3.7V/2.6Ah$) are set up as Fig. 6. Battery cells are implemented by Thévenin equivalent circuit models in Typhoon HIL 602+ and are configured as follows: The initial SOC of every cell is set to 100% but the internal resistance is configured as different as in Table I. The balancing capacitance, C, and the sum of on-resistance of the switch and internal resistance of capacitor are set to $1000\mu F$ and $100m\Omega$, respectively. To fully discharge the capacitor, the dummy load, R_{dummy}, is designed as $20m\Omega$ by (13). The switching frequency is regulated from $100Hz$ to $10kHz$ to measure the battery impedance.

The testing is divided into low-frequency and frequency-sweep tests. At first,a $100Hz$ low-frequency examinations are used to validate the measurement accuracy. The waveforms of battery voltage and current presented in Fig. 7(a) comply with the operation analysis in Section II-B. Each battery resistance

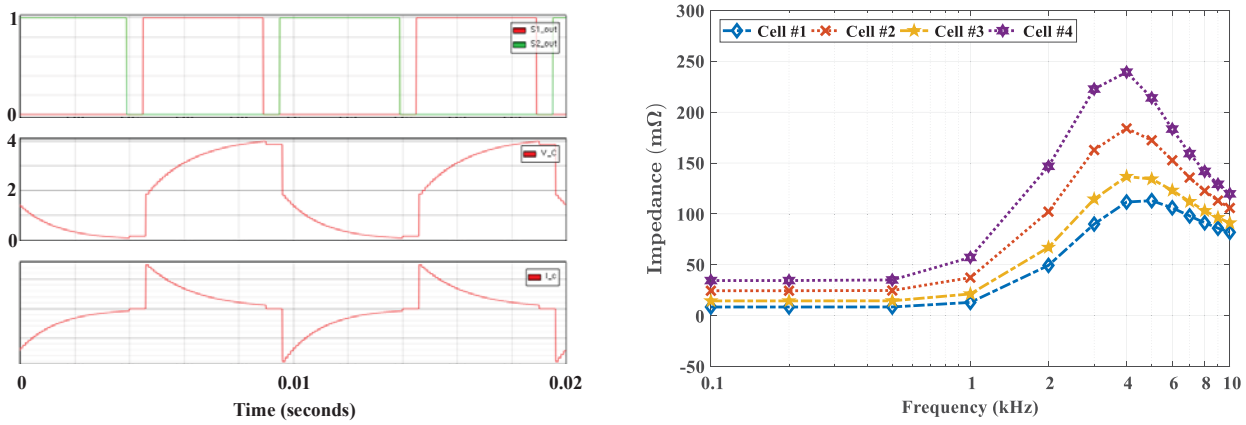

(a) (b)

Fig. 7: Real-time simulation results: (a) capacitor voltage and current waveform; (b) battery impedance of cells in frequency-sweep examination.

TABLE I: Battery resistance estimation in 100Hz switching frequency

	Actual value ($m\Omega$)	Estimation Results						Measurement Error (%)
		Sampling #1($m\Omega$)	Sampling #2($m\Omega$)	Sampling #3($m\Omega$)	Sampling #4($m\Omega$)	Sampling #5($m\Omega$)	Average ($m\Omega$)	
Cell #1	24	25.95	25.87	25.95	25.88	20.18	24.77	3.2
Cell #2	40	38.62	40.25	39.88	41.12	42.30	40.44	1.1
Cell #3	30	32.74	29.25	33.12	30.51	31.69	31.46	4.87
Cell #4	50	48.36	51.72	49.67	50.29	52.32	50.47	0.94

is scanned 5 times and then those are averaged. The measured resistance of the cells are compared with the initial setup in Table I. The differences between the measured resistance and actual value are within 5%. Thus, the online EIS measuring scheme can be adopted for the real applications.

On the other hand, the frequency-sweep examinations assess the dynamic characteristic of the battery cell under various operating frequency. While the operating frequency is swept from $100Hz$ to $10kHz$, the corresponding impedance at each frequency is measured. The measured data is plotted in Fig. 7(b), which shows that the cell resistance depends on the frequency. Such a battery resistance can be utilized to estimate the SOC and its degradation with time elapse is useful for the SOH estimation.

Conclusion

This paper proposes an online impedance spectroscopy measurement scheme that can be merged with the switch-matrix flying capacitor equalizer. The switch-matrix structure helps the measurement circuit to directly assess the impedance of every cell by a slight modification of the original circuit with a small extra system cost. According to the real-time simulation results, the measurement error is only within 5% in the low-frequency examinations. Furthermore, because the impedance estimation process is activated only when it is required, it does not disturb the normal cell balancing operation. Even though the proposed method can measure only the real part of the complex battery impedance, an improved algorithm to obtain the imaginary part of the impedance will be presented in our next paper.

Acknowledgment

This work was supported by the National Research Foundation of Korea (NRF) grant funded by the Korea government (MSIT) (*NRF-2020R1A2C2009303*).

References

[1] R. Koch, R. Kuhn, I. Zilberman, and A. Jossen, "Electrochemical impedance spectroscopy for online battery monitoring - power electronics control," 2014 16th European Conference on Power Electronics and Applications, Lappeenranta, 2014, pp. 1-10, DOI: 10.1109/EPE.2014.6910907.

[2] T.-T. Nguyen, V.-L. Tran and W.-J. Choi, "Development of the intelligent charger with battery State-Of-Health estimation using online impedance spectroscopy," 2014 IEEE 23rd International Symposium on Industrial Electronics (ISIE), Istanbul, 2014, pp. 454-458, DOI: 10.1109/ISIE.2014.6864656.

[3] S. Cho, I. Lee, J. Baek and G. Moon, "Battery Impedance Analysis Considering DC Component in Sinusoidal Ripple-Current Charging," in IEEE Transactions on Industrial Electronics, vol. 63, no. 3, pp. 1561-1573, March 2016, DOI: 10.1109/TIE.2015.2497661.

[4] E. Din, C. Schaef, K. Moffat, and J. T. Stauth, "A Scalable Active Battery Management System With Embedded Real-Time Electrochemical Impedance Spectroscopy," in IEEE Transactions on Power Electronics, vol. 32, no. 7, pp. 5688-5698, July 2017, DOI: 10.1109/TPEL.2016.2607519.

[5] M. A. Varnosfaderani and D. Strickland, "Online impedance spectroscopy estimation of a dc-dc converter connected battery using a switched capacitor-based balancing circuit," in The Journal of Engineering, vol. 2019, no. 7, pp. 4681-4685, 7 2019, DOI: 10.1049/joe.2018.8069.

[6] P.-H. La, H.-H. Lee, and S.-J. Choi, "A Single-Capacitor Equalizer Using Optimal Pairing Algorithm for Series-Connected Battery Cells," 2019 IEEE Energy Conversion Congress and Exposition (ECCE), Baltimore, MD, USA, 2019, pp. 5078-5083, DOI: 10.1109/ECCE.2019.8913276.

[7] Seaman, Aden, Thanh-Son Dao, and John McPhee. "A survey of mathematics-based equivalent-circuit and electrochemical battery models for hybrid and electric vehicle simulation." Journal of Power Sources 256 (2014): 410-423.

APEC 2021
VIRTUAL CONFERENCE + EXPOSITION

T25.6

Integrated On-Line EIS Measurement Scheme Utilizing Flying Capacitor Equalizer for Series Battery String

JUNE 9th – 17th, 2021

Phuong-Ha La* and Sung-Jin Choi
University of Ulsan, Republic of Korea

Contents

- Introduction
- Conventional methods
- Proposed method
- Verifications
- Conclusion

1. Introduction: Research Motivation

- Battery cells are **screened** and **sorted** before the **assembly**.
- Battery cells are connected **in series** to increase the voltage range.
- The characteristics of battery cells are so **different** that it may cause:
  - **Ineffective utilization** of the available capacity
  - Possible **over-charge** and **over-discharge** of the battery cells

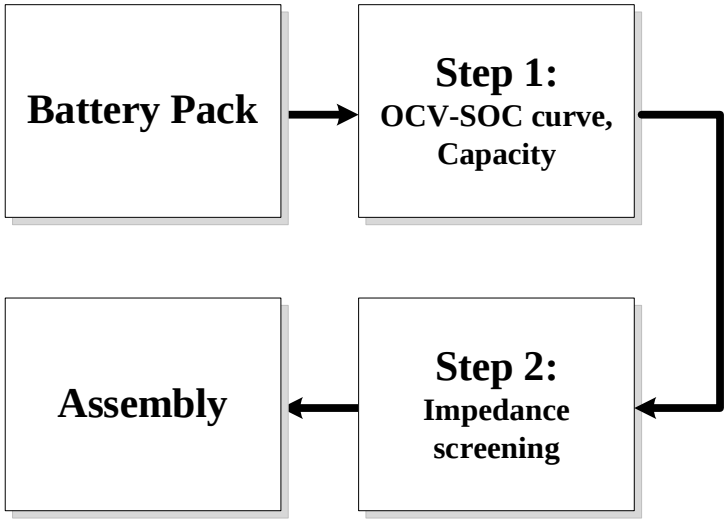

Cell-screening process

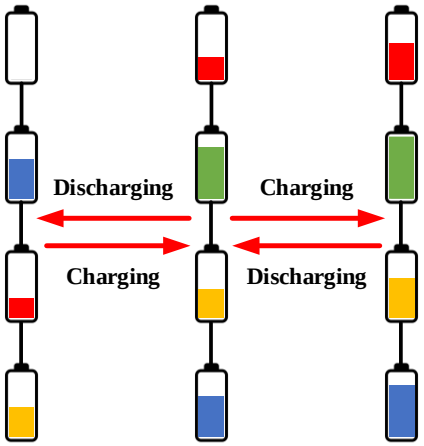

SOC inconsistency during charging/discharging

1. Introduction: Research Motivation

- Even in the **same operating conditions**, the **performance degradation** of individual cells are **different**.
- If the system **lacks individual-cell state (SOC, SOH) monitoring** and cell balancing methods, the available capacity of system is further reduced.

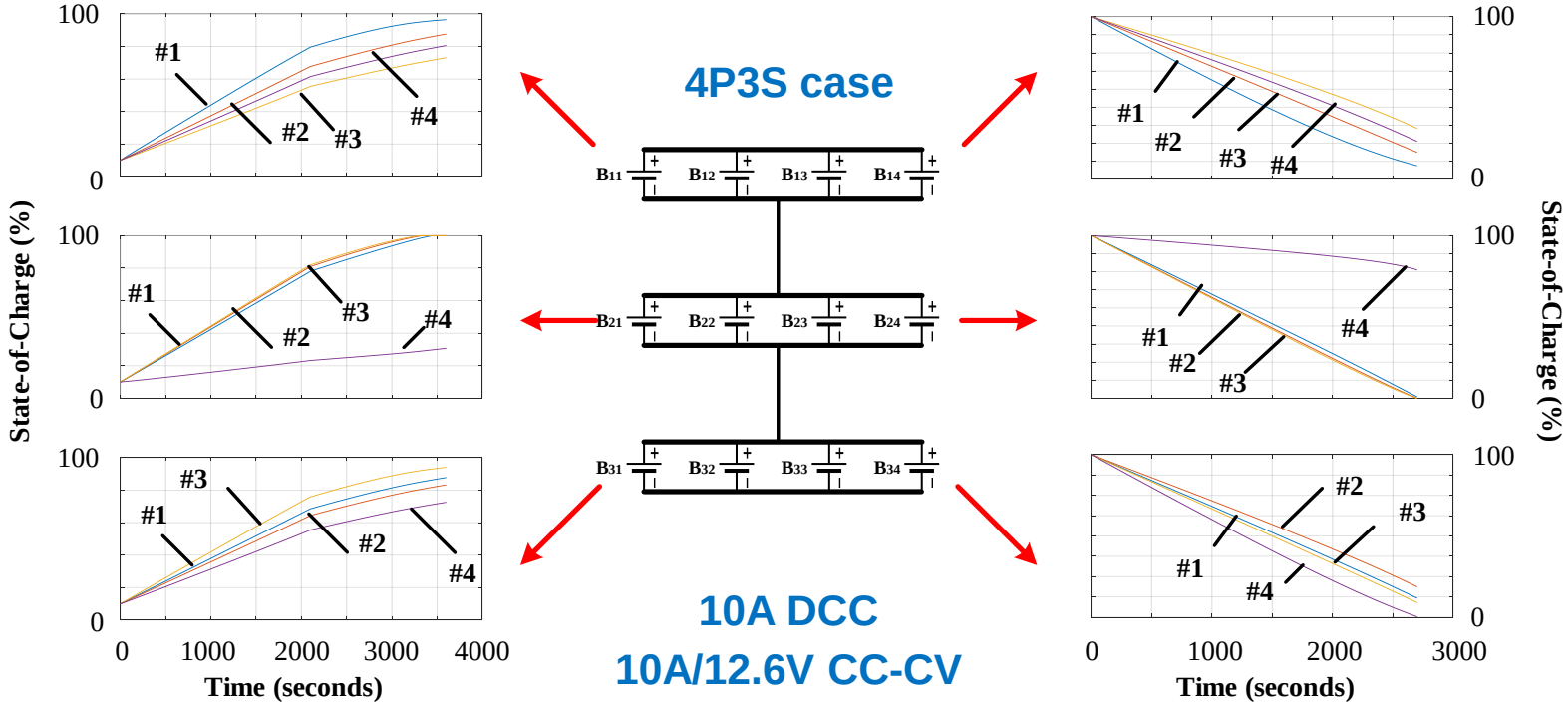

1. Introduction: Research Motivation

- **Battery lifetime can be assessed by various ways:**
  - **Ratio** between the **actual capacity** and the **initial capacity**
  - → It requires a **long measurement time** to complete the cycle.
  - Trend of **impedance change**
  - → Fast and suitable for individual-cell estimation

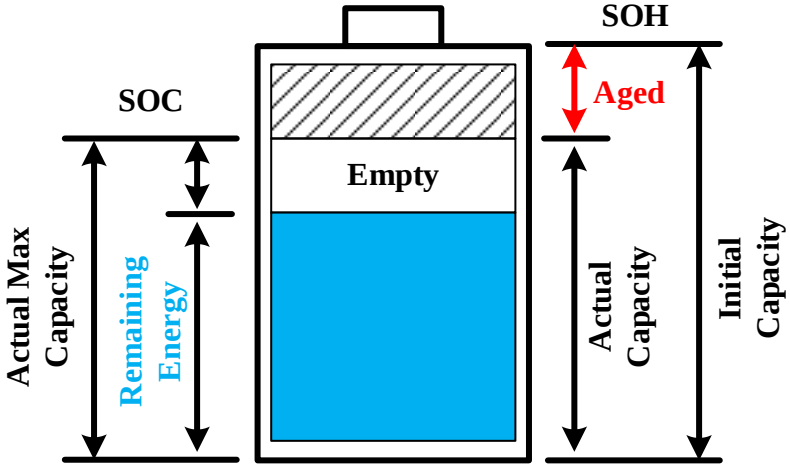

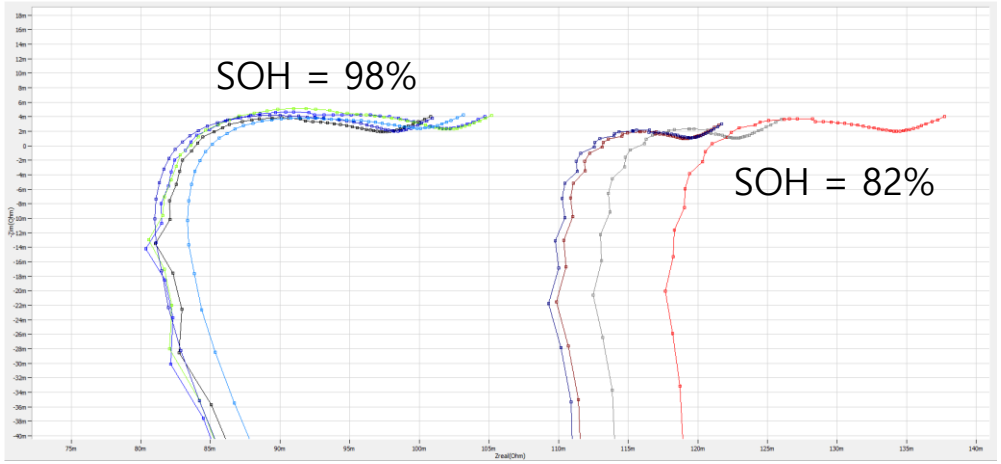

$$SOH = 100\frac{Actual\ Capacity}{initial\ Capacity}$$

$$SOH = f(Z)$$

2. Conventional Method

- Sinusoidal **voltage (Galvano-static)** or **current (Potentio-static)** signal is **injected** to the battery to observe **current** or **voltage** response.
- The **magnitudes and phase angles** of the signals are analyzed to get the Impedance plot (Nyquist plot).
- Curve fitting methods are used to derive the circuit parameters for the equivalent circuit.

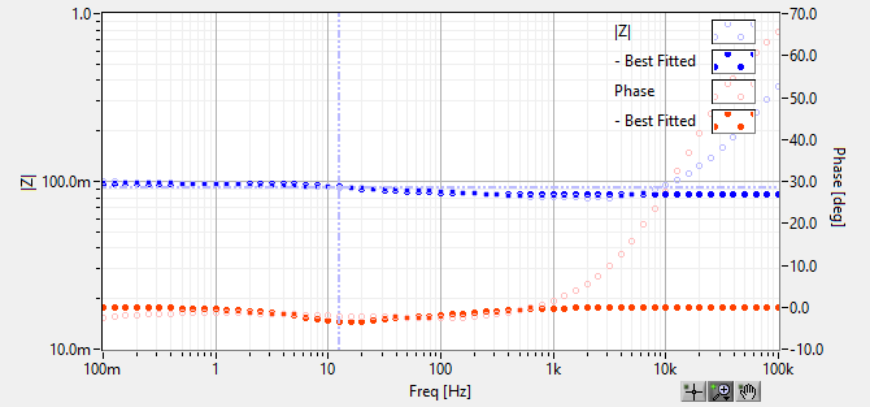

Bode Plot from Zive EIS

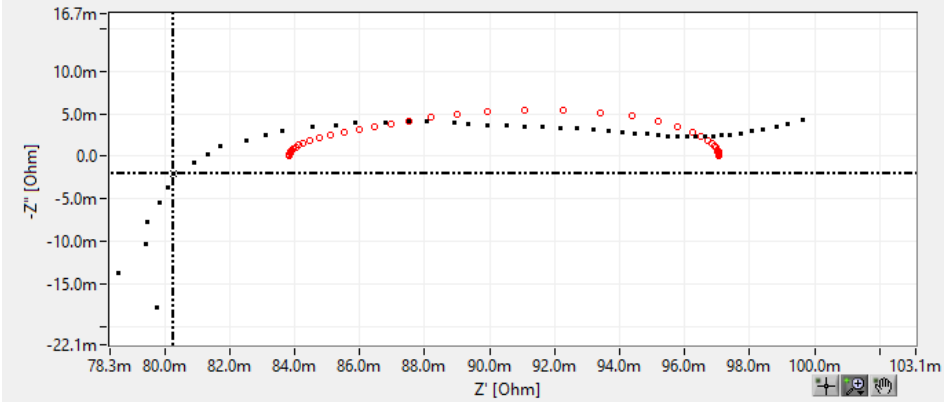

Nyquist Plot from Zive EIS

2. Conventional Methods

- **Since integration** of the **EIS scheme** into charger[2] or balancing circuit[4] has many **advantages**, there has been a few previous researches.
- **Fundamental problems** of the conventional methods:
  - Only feasible to whole battery pack.
  - **Higher costs** for **individual cell estimation**.
  - **Accuracy-dependency** on the **sinusoidal waveform quality**.
  - **Unknown risks** during the **sinusoidal signal injection**.

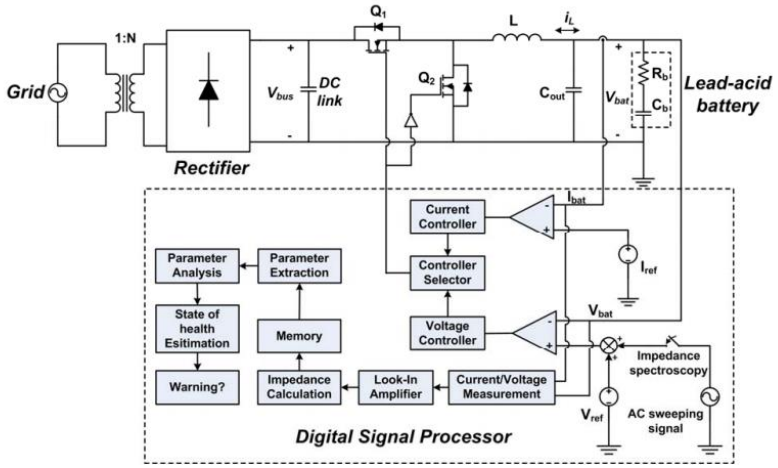

Integrated EIS function to charger [2]

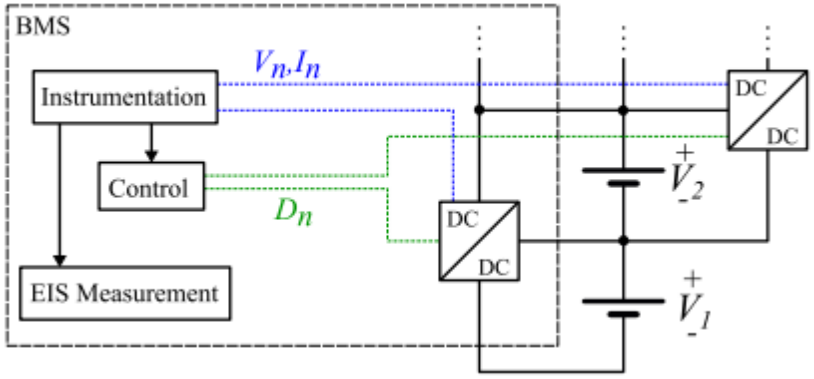

Integrated EIS function to balancing circuit [4]

3. Proposed Method: Topology

➢ **Circuit configuration:**

- **Simple circuit {1 switch, 1 resistor, and 1 voltage sensor}** is added to **conventional Switch-matrix single capacitor equalizer**.
- **Balancing capacitor, C,** is reused as a part of estimation circuit.
- The $\mathbf{R_{dummy}}$ discharges the balancing capacitor before each measuring process.
- **Switch-matrix** alternatingly connects **each battery cell** to **capacitor C**.
- **Battery impedance** is measured based on **charge transfer mechanism** of **switched capacitor converter**.

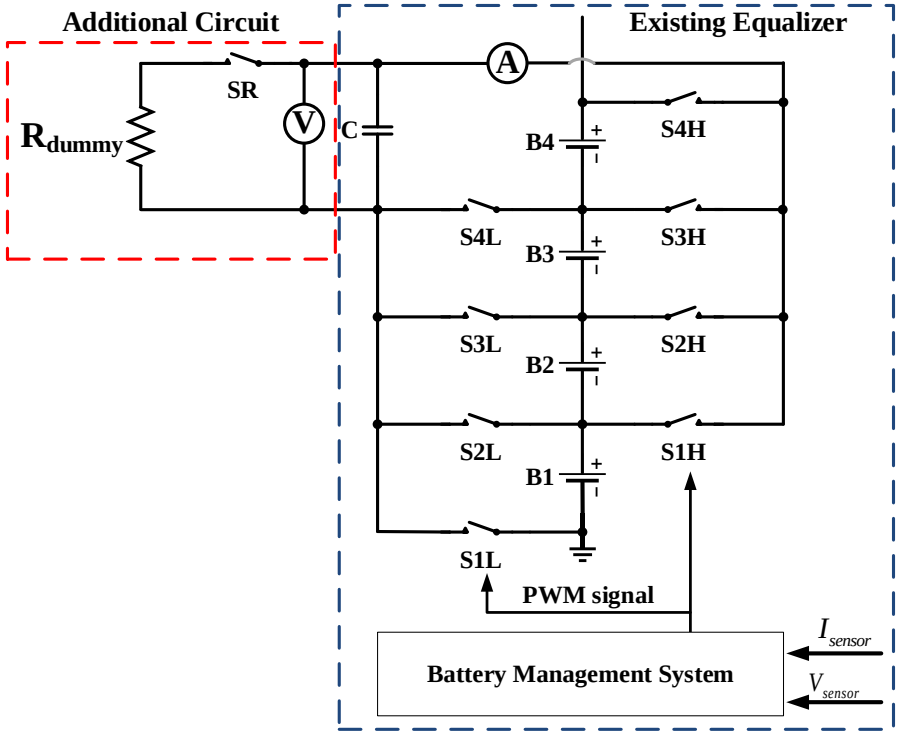

3. Proposed method: Measurement process

- **Measurement process** is divided into **2 phases**:
  - **Charge transfer phase:** from t_0 **to** t_1, battery **transfer charge** to capacitor, C.
  - **Calibration phase:** from t_2 **to** t_3, discharge capacitor, C, by R_{dummy}.

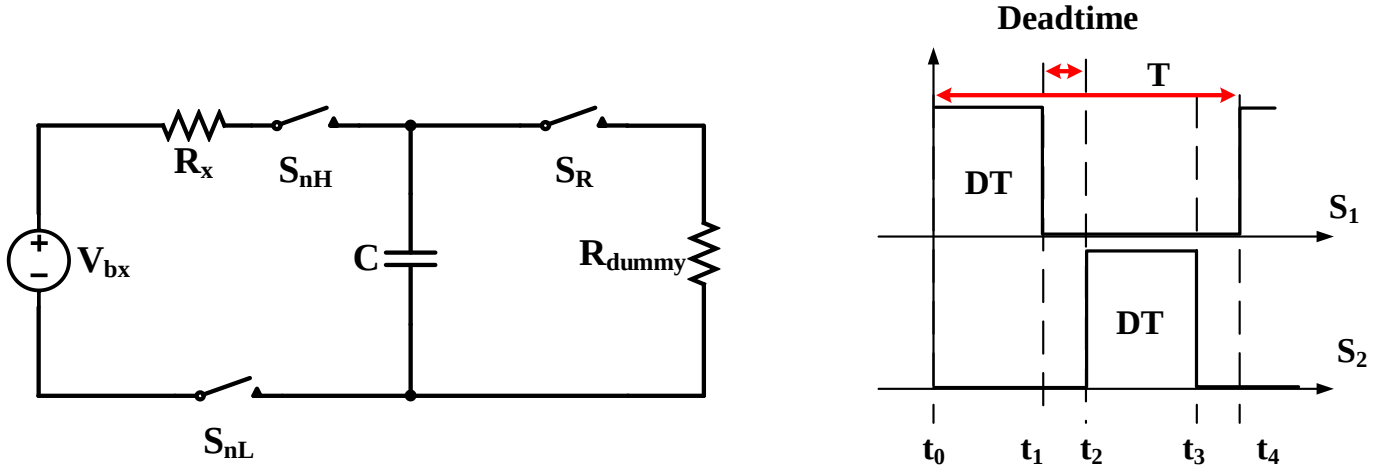

Equivalent circuit

$$\tau_1 = R_x C \qquad (1)$$

$$R_x = Z_{bx} + R_{d,on} + ESR \qquad (2)$$

Denote Z_{bx} is impedance of battery, $R_{d,on}$ is the on resistance of switches, **ESR** is internal resistance of balancing capacitor.

3. Proposed method: Charge Transfer Phase

- Switches **S_mH** and **S_mL** are turned on.
- **Balancing capacitor, C**, is charged by the **battery cell**.

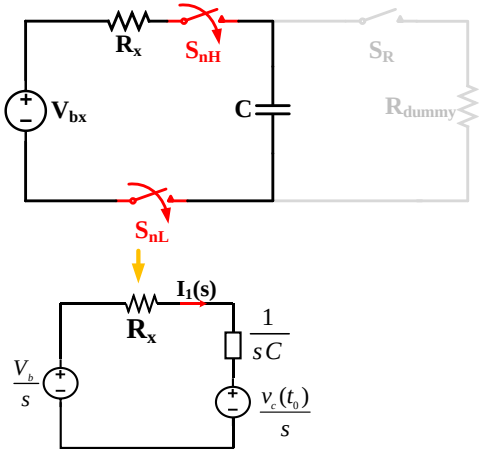

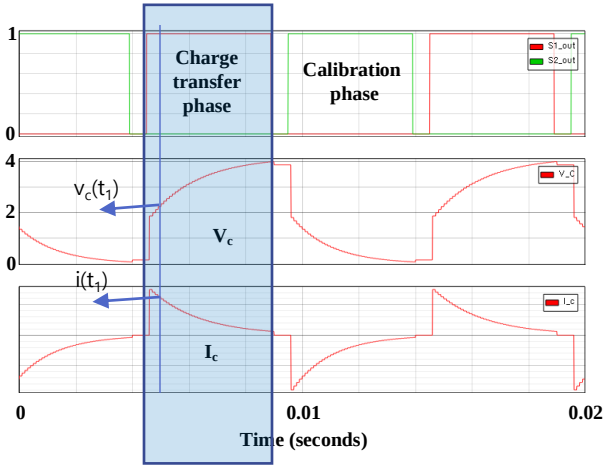

- The **charging current** in time-domain and the increased charge during **charge transfer phase**:

$$i_1(t) = \frac{\Delta V}{R_x} e^{\frac{-t}{\tau_1}} \quad (5)$$

$$Q_{in}(t_1) = \int_{t_0}^{t_1} i_1(t)dt = \Delta V \left(1 - e^{\frac{-t_1}{\tau_1}}\right) C \quad (6)$$

- The **capacitor voltage** at the **end of charging time**:

$$v_c(t_1) = \frac{Q_{in}}{C} = \Delta V(1 - e^{\frac{-t_1}{\tau_1}}) + v_c(t_0) \quad (7)$$

3. Proposed method: Charge Transfer phase

- **Impedance of battery is estimated in Charge transfer phase**
- The impedance of battery is estimated by solving (11).

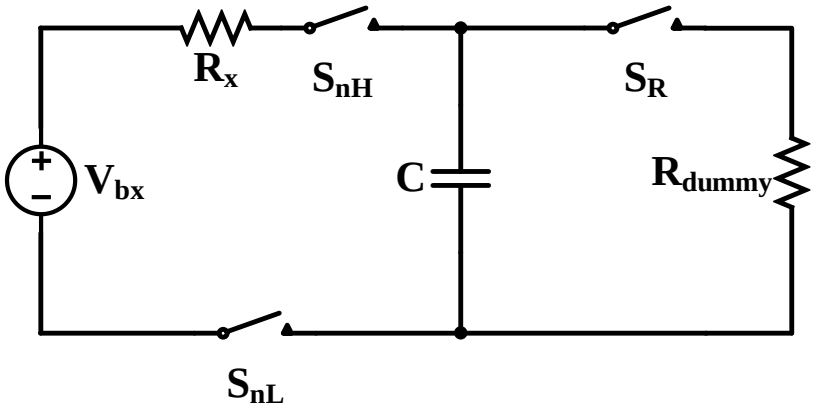

Denote ***Z_{bx}*** *is impedance of battery,* ***$R_{d,on}$*** *is the on resistance of switches,* ***ESR*** *is internal resistance of balancing capacitor.*

$$R_x = Z_{bx} + R_{d,on} + ESR \quad (2)$$

$$\frac{i(t_1)}{v_c(t_1)} = \frac{1}{R_x}\frac{e^{\frac{-t_1}{R_x C}}}{\left(1 - e^{\frac{-t_1}{R_x C}}\right)} \quad (8)$$

$$G_x = \frac{1}{R_x} \quad (9)$$

$$f(G_x) = G_x \frac{e^{\frac{-G_x t_1}{C}}}{1 - e^{\frac{-G_x t_1}{C}}} - \frac{i(t_1)}{v_c(t_1)} \quad (10)$$

$$G_x(i+1) = G_x(i) - \frac{f(G_x(i))}{f'(G_x(i))} \quad (11)$$

$$Z_{bx} = \frac{1}{G_x(i+1)} - R_{d,on} - ESR \quad (12)$$

3. Proposed method: Calibration phase

- In **Calibration phase**, **balancing capacitor** is discharged by **dummy resistor**.
- **Dummy resistor** is designed to provide **sufficient discharge** of the stored charge in the capacitor:

$$R_{dummy} \leq \frac{1}{5 f_{s\_max} C} \qquad (13)$$

Denote $\mathbf{f_{s\_max}}$ is the maximum frequency in the swept-frequency range.

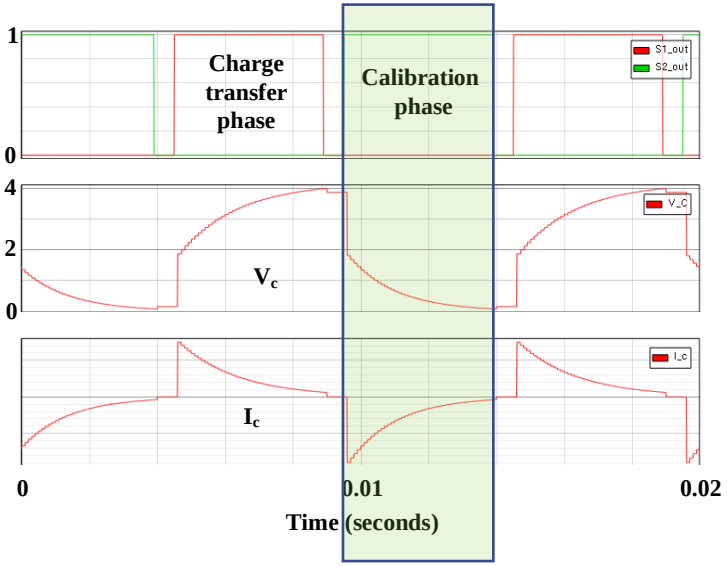

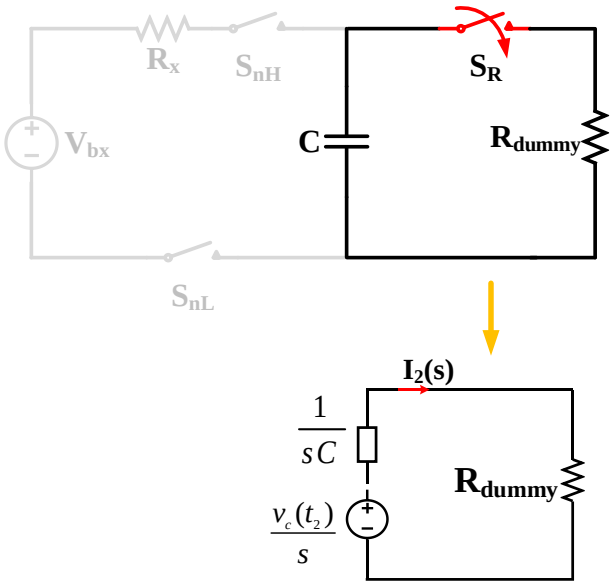

3. Proposed method: Overall Operation Principle

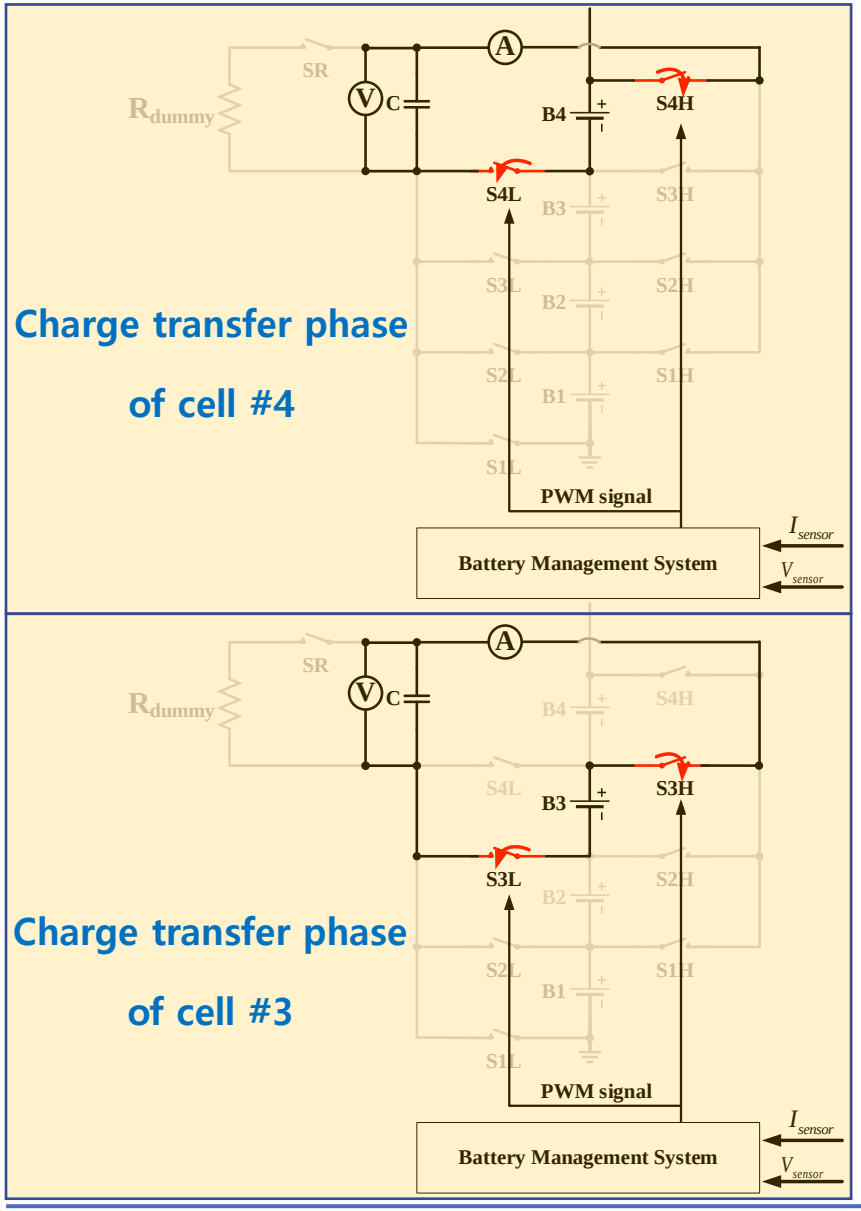

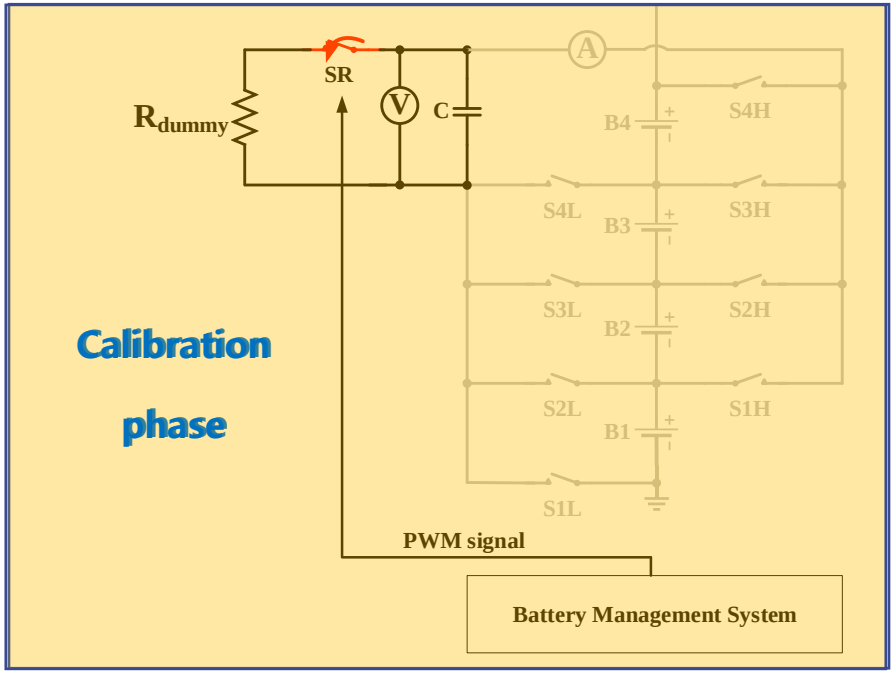

4. Verification: Test setup

- **Real-time simulation** test setup are prepared for an **4S1P battery configuration** of 18650 Li-ion battery cells (3.6V – 2600mAh).
- Thévenin model of battery is used to arbitrarily choose the impedance parameters.
- The **internal resistance** and **capacitance** of the **switch-matrix single capacitor balancing circuit** is assumed to be **100mΩ** and **1000uF** (designed for balancing circuit in [6]).
- The **switching frequency** is swept from 100Hz to 10kHz.

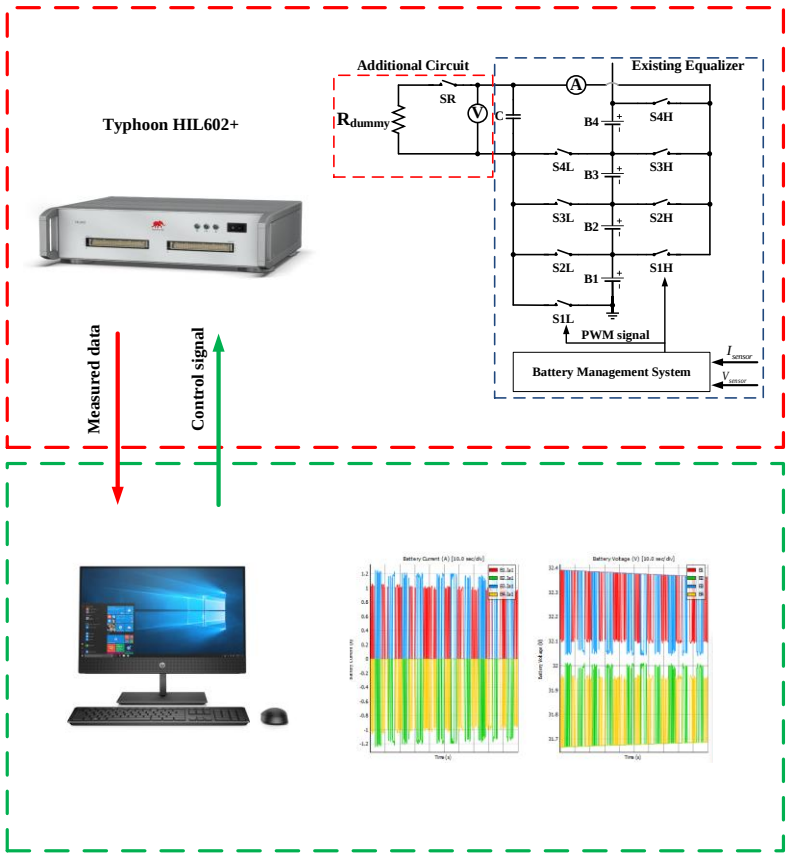

Test setup

4. Verification: Low-frequency Test Results

- At first, **low-frequency examination (f_s = 100Hz)** is performed to assess the **accuracy of the measurement**.
- The measurement is **repeated 5 times** to reduce the influence of noises.
- **Measurement error** is within **5%**.

TABLE I: Battery resistance estimation in 100Hz switching frequency

	Actual value ($m\Omega$)	Estimation Results						Measurement Error (%)
		Sampling #1($m\Omega$)	Sampling #2($m\Omega$)	Sampling #3($m\Omega$)	Sampling #4($m\Omega$)	Sampling #5($m\Omega$)	Average ($m\Omega$)	
Cell #1	24	25.95	25.87	25.95	25.88	20.18	24.77	3.2
Cell #2	40	38.62	40.25	39.88	41.12	42.30	40.44	1.1
Cell #3	30	32.74	29.25	33.12	30.51	31.69	31.46	4.87
Cell #4	50	48.36	51.72	49.67	50.29	52.32	50.47	0.94

4. Verification: Swept-frequency Test Results

- **Swept-frequency** measurement is taken to assess the **dynamic characteristics** of battery cells under **various PWM pulse frequencies**.
- Battery impedance is estimated at **10 frequencies** in the range from **100Hz to 10kHz**.

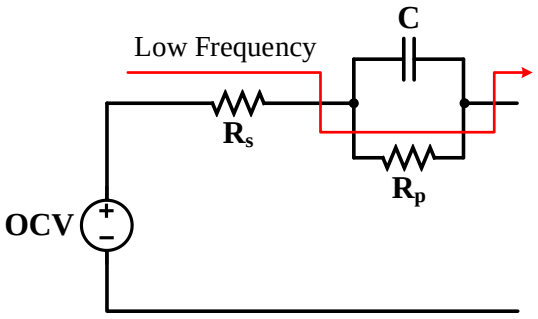

Characteristic of battery in low f_s

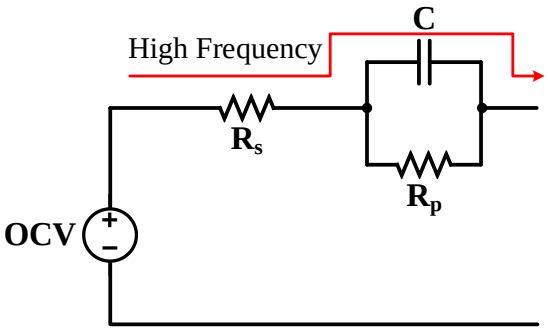

Characteristic of battery in high f_s

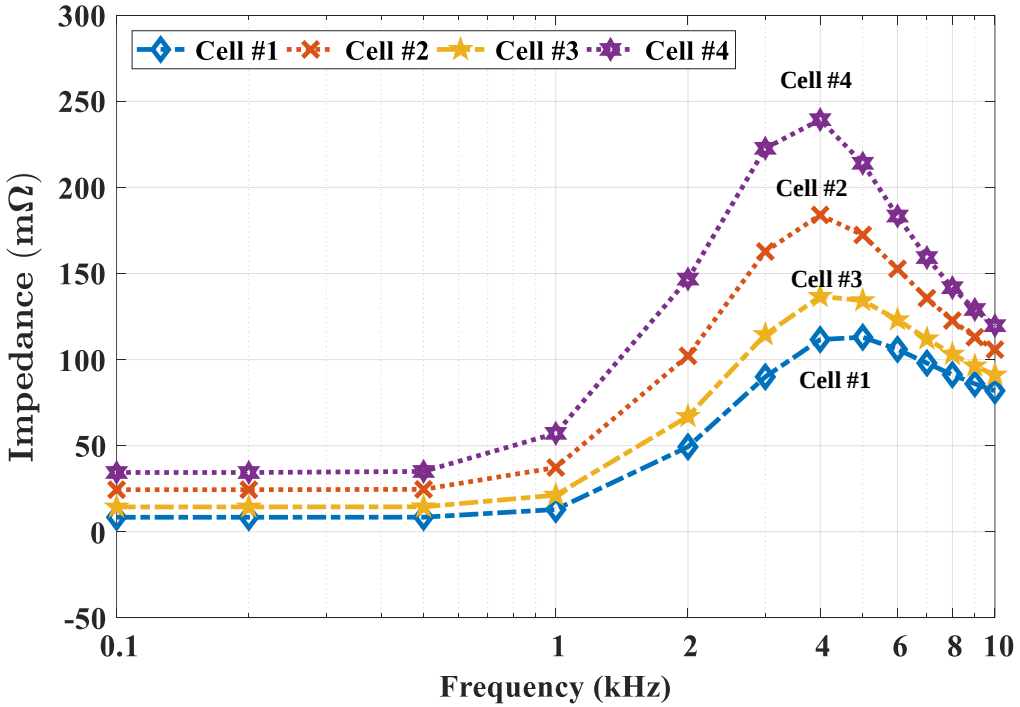

Impedance estimation according to Swept-frequency test

5. Conclusions

- **This paper proposes a compact online EIS measurement circuit for series-connected battery cells, which has the following merits:**
  - It is **easily integrated** into the **existing switch-matrix cell balancing circuit**.
  - It **does not disturb** the **original balancing operation** by utilizing the **idle time** of the balancing circuit.
  - Only **few circuit components** are added. (Existing balancing capacitor is reused.)
  - **Individual cell impedances** are estimated with **high accuracy** (within **5%** in the low-frequency test).
  - By sweeping the switching frequency, the **frequency characteristics of cell impedance** can be assessed.
- **Future works:**
  - **Hardware experiments** will be prepared to further verify the performance of proposed method.
  - An improved algorithm to obtain **not only the magnitude but also the phase of cell impedance** is under development.

THANK YOU FOR YOUR ATTENTION

Contact information for more detail:

Phuong-Ha La

Email: ***laphuongha@gmail.com***

URL: **http://eccl.ulsan.ac.kr/**